DAMAGE STATE PROBABILITY ESTIMATION FOR SEISMIC LIFE CYCLE COST OF RETROFITTED RC STRUCTURES WITH SELF-CENTERING SYSTEM

M. Noureldin[1], J. Kim[2]

[1] *Assistant Professor, Sungkyunkwan Univ., m.nour@skku.edu*
[2] *Professor, Sungkyunkwan Univ., jkim12@skku.edu*

Abstract

In this study, a seismic Life-Cycle Cost (LCC) evaluation is used to assess the seismic performance of RC structures retrofitted with self-centering post-tensioned pre-cast concrete (SC-PC) frame with enlarged beam-ends. The seismic LCC is estimated for the retrofitted and un-retrofitted structures using damage state probability. The probabilities of exceedance for three different damage states are obtained through a fragility function using thirty different natural earthquake records. For the seismic fragility calculation, the dispersion in demand is obtained based on conducting numerous nonlinear time history (NLTH) response analyses of the model structure. A five-story reinforced concrete moment resisting frame building is used as a case study. The proposed retrofitting scheme found to be effective in reducing the total damage cost of the retrofitted structure investigated in the current study, especially, when the retrofitting scheme has low initial cost compared to the expected life-long total damage cost of the building.

Keywords: Seismic Life-Cycle Cost, Seismic fragility, Seismic performance, Self-centering system.

1. Introduction

Many existing buildings severely damaged during recent earthquakes due to the deficiency of proper seismic detailing. This is primarily attributed to the lack of knowledge related to the seismicity of the building location and the less accumulated seismic knowledge at the time of the design and construction of the building. This fact necessitates retrofitting and upgrading of the existing buildings to cope up with the modern seismic codes and guidelines. After retrofitting, the retrofitted building needs to be seismically evaluated to assess the effectiveness of the proposed retrofit.

Seismic retrofitting using self-centering (SC) systems proved to be an effective upgrading system for existing structures [1, 2, 3]. SC system has been applied to structures, such as RC buildings [e.g. 4], steel buildings [e.g. 5, 6], and bridge piers [e.g. 7]. Recently, smart materials have been applied to SC systems, for example, Wang and Zhu [8] experimentally investigated the application of shape-memory alloy to a self-centering system. Dezfuli et al [9] conducted a parametric study on an innovative Core-Less Self-Centering (CLSC) brace and investigated the optimum cost of materials involved, in addition to achieving a full self-centering behavior. Ryotaro et al. [10] conducted cyclic loading tests on precast prestressed concrete with SC system and cast-in-situ reinforced concrete frame subassemblies to demonstrate the effectiveness of SC system in the control of cracking. Rare studies investigated the effectiveness of the SC system from the life-cycle cost (LCC) perspective [11].

In the current study, a seismic LCC evaluation is investigated for an RC structure retrofitted with an exterior self-centering post-tensioned pre-cast concrete (SC-PC) frame with enlarged beam-ends. The SC-PC frame is added to the exterior frames of the building from the outside to avoid stopping the functionality of the building. The retrofitted building is shown in Fig. 1, and the connection between the beam and column of the SC-PC frame is shown in Fig. 2.
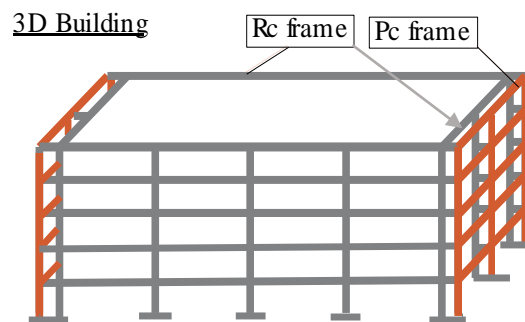

Fig. 1- 3-D RC building retrofitted with a self-centering PC frame [19].
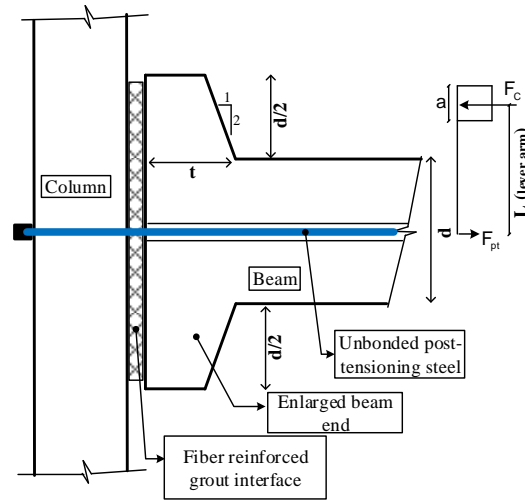
Fig. 2 - Details of the beam-column connection of self-centering-PC Frame [19].

2. Mathematical modeling of the SC-PC frame

In order to increase the capacity of the beam-column connection of the SC-PC frame, the depth of the PC beam-ends is enlarged as shown in Fig. 2

Celik and Sritharan [12] showed that for grade 270 prestressing strands, the stress-strain relation of the post-tensioning tendon can be given as,

$$f_{pt} = \varepsilon_{pt}.E_p.\left[0.02 + 0.98 \Big/ \left[1 + \left(\frac{\varepsilon_{pt}.E_p}{1.04 \cdot f_{py}}\right)^{8.36}\right]^{1/8.36}\right] \tag{1}$$

where E_p is the elastic modulus of the prestressing steel; ε_{pt} is the strain in the post-tensioning tendon; f_{py} is the yield strength of the post-tensioning tendon.

The moment capacity of the PC beam-column connection is calculated as follows [Fig. 2],

$$M_{cap} = F_{pt} \cdot (h_g - a)/2 \tag{2}$$

Where M_{cap} is the moment capacity of the beam-column connection, F_{pt} is the force developed in the post-tensioning tendon, h_g is the depth of the grout pad at the beam-column interface, a is the depth of the equivalent rectangular compression stress block corresponding to the compression force, which can be determined using the following equation [13]:

$$a = F_c/0.85 \, f_c' \, b_g \tag{3}$$

3

where F_c is the concrete compression force; b_g is the width of the grout pad at the beam-column interface; f'_c is the unconfined concrete compression strength. At yield of the post-tensioning tendon, M_{cap} can be calculated as,

$$M_{cap} = F_{py} \cdot (h_g - a)/2 \tag{4}$$

The decompression point defines the beginning of a gap opening at the beam-column interface. Due to the pre-compression developed by the initial prestressing force, the following equation is used to determine the moment resistance at gap opening, $M_{decomp,}$ [12].

$$M_{decomp} = f_{pi} \cdot I/(\frac{h_g}{2}) \tag{5}$$

where f_{pi} is the initial stress in the post-tensioning tendon; I is the moment of inertia of the beam section based on the gross section properties; h_g is the height of the grout pad at the interface.

A bi-linear elastic spring is used to model the gap opening between the column and the beam at the decompression level in the PT tendons. When the applied moment exceeds M_{decomp}, the PT tendons start to elongate allowing the gap to increase.

3. A five-story case study building

Fig. 3 shows the bare and SC-PC frames used in the current study. The cross-section dimensions of the bare frame beams are 250mm x 500mm; for columns are 400 mm x 400 mm. The longitudinal reinforcement bars have 413 MPa yield strength. 4D20 and 8D16 bars are used for beams and columns, respectively, with D8 @ 150mm transverse reinforcement. The compressive strength of the concrete is 21 MPa. The bare building is designed for gravity loads only with 7.0 and 2.0 kN/m² for dead and live loads, respectively. ASCE/SEI-41 [14] is used to define the plastic hinges for the beam and column section. A 2-D frame is permitted to be used instead of the 3-D model [14] as long as there is a rigid diaphragm connecting all frames and there is no irregularity in the building.

The initial stress after losses, f_{pi}, of the tendon is 820 MPa and the yield strength of the post-tensioning tendons of the SC-PC frame, f_{py}, is 1,757 MPa. The nominal compressive strength of concrete, f'_c, is 34.0 MPa and the grout compressive strength is taken as 64.0 MPa. The tendon area is 380.0 mm² and the PC beam and column sections are 300 by 600 mm and 400 by 400 mm, respectively. The SC-PC frame is rigidly connected to the bare frame laterally. The connection between the bare frame and the retrofitting frame should be rigidly connected laterally at the connection between the beam and column.
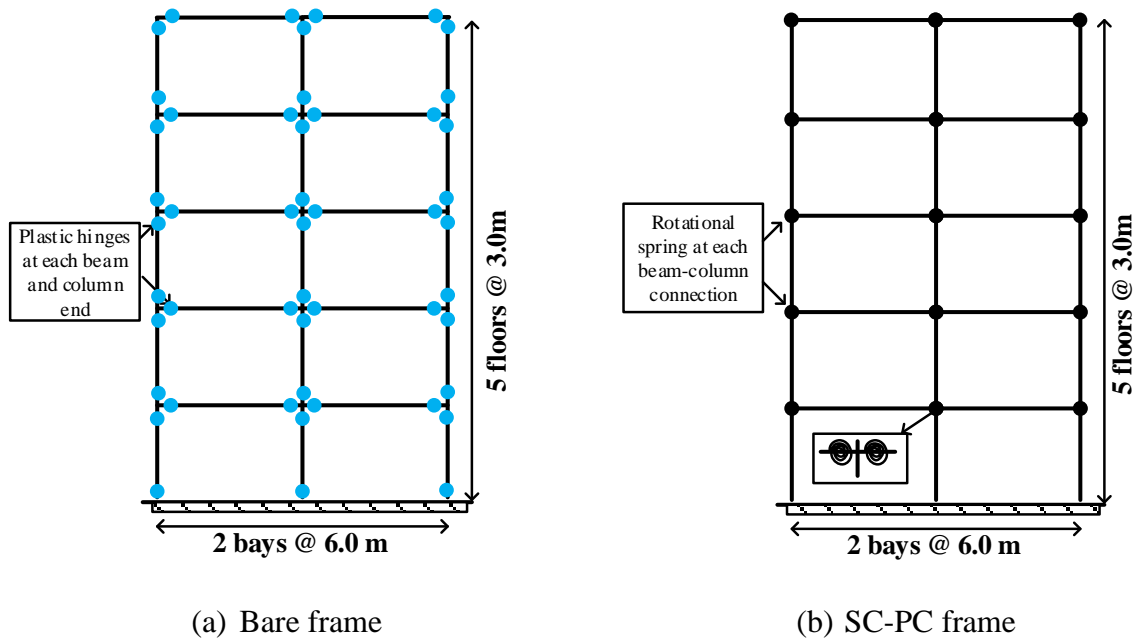
4

(a) Bare frame (b) SC-PC frame

Fig. 3- Bare frame and the SC-PC frame analytical models [19].

4. Earthquake records, incremental dynamic analysis (IDA), and fragility curves (FC)

In this section, extensive non-linear time history response (NLTH) analyses are conducted using Sap2000 [15] to construct the IDA and fragility curves, which will be used for estimating the seismic LCC in the next section. Thirty-earthquake ground-motion records are extracted from PEER NGA Database [16] and listed in Table 1 are used to construct the IDA curves. Fig. 4 shows the response spectra of the ground motions.

For conducting the NLTH analyses, the beams and columns are modeled using the frame elements in the Sap2000 library. For the SC-PC frame, a multi-linear elastic link at the connection between the beam and column is used. For the bare frame, a rigid connection is defined at the beam-column interface.

Table 1. List of the earthquake records used in constructing the IDA curves.

PEER Record Sequence Number	Earthquake Name	Station Name	Magnitude
68	"San Fernando"	"LA - Hollywood Stor FF"	6.61
125	"Friuli_ Italy-01"	"Tolmezzo"	6.5
169	"Imperial Valley-06"	"Delta"	6.53
174	"Imperial Valley-06"	"El Centro Array #11"	6.53
721	"Superstition Hills-02"	"El Centro Imp. Co. Cent"	6.54
725	"Superstition Hills-02"	"Poe Road (temp)"	6.54
752	"Loma Prieta"	"Capitola"	6.93

5

| 767 | "Loma Prieta" | "Gilroy Array #3" | 6.93 |
828	"Cape Mendocino"	"Petrolia"	7.01
848	"Landers"	"Coolwater"	7.28
900	"Landers"	"Yermo Fire Station"	7.28
953	"Northridge-01"	"Beverly Hills - 14145 Mulhol"	6.69
960	"Northridge-01"	"Canyon Country - W Lost Cany"	6.69
1111	"Kobe_ Japan"	"Nishi-Akashi"	6.9
1116	"Kobe_ Japan"	"Shin-Osaka"	6.9
1148	"Kocaeli_ Turkey"	"Arcelik"	7.51
1158	"Kocaeli_ Turkey"	"Duzce"	7.51
1244	"Chi-Chi_ Taiwan"	"CHY101"	7.62
1485	"Chi-Chi_ Taiwan"	"TCU045"	7.62
1602	"Duzce_ Turkey"	"Bolu"	7.14
1633	"Manjil_ Iran"	"Abbar"	7.37
1787	"Hector Mine"	"Hector"	7.13
12	"Kern County"	"LA - Hollywood Stor FF"	7.36
22	"El Alamo"	"El Centro Array #9"	6.8
30	"Parkfield"	"Cholame - Shandon Array #5"	6.19
38	"Borrego Mtn"	"LB - Terminal Island"	6.63
121	"Friuli_ Italy-01"	"Barcis"	6.5
126	"Gazli_ USSR"	"Karakyr"	6.8
138	"Tabas_ Iran"	"Boshrooyeh"	7.35
280	"Trinidad"	"Rio Dell Overpass - FF"	7.2
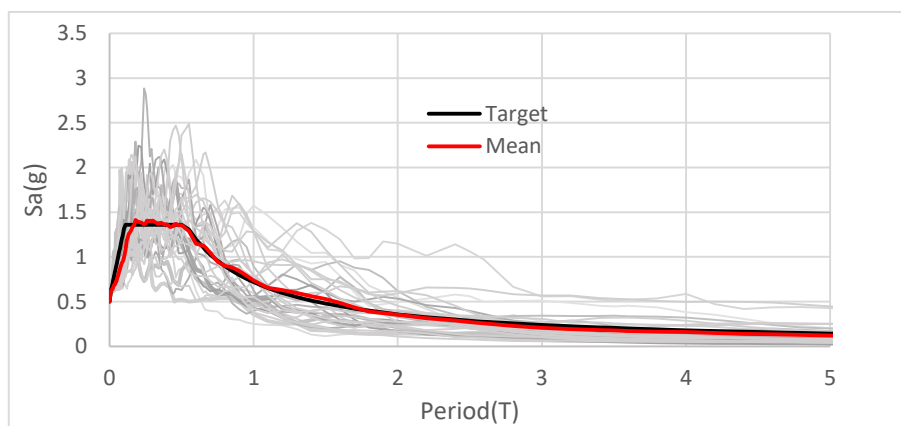
Fig. 4 The 30 response spectra of the ground motion records used for IDA.

IDA curves are constructed by conducting NLTH analyses for the selected ground motions scaled to a specific intensity-measure in increasing order until dynamic instability is encountered. Fig. 5 shows the IDA curves for the bare and retrofitted frames. Each dot on the IDA curve represents the response of an earthquake

6

2j-0013

scaled to the specific intensity level. The figure shows that the retrofitted frame has better seismic performance compared to the bare one.

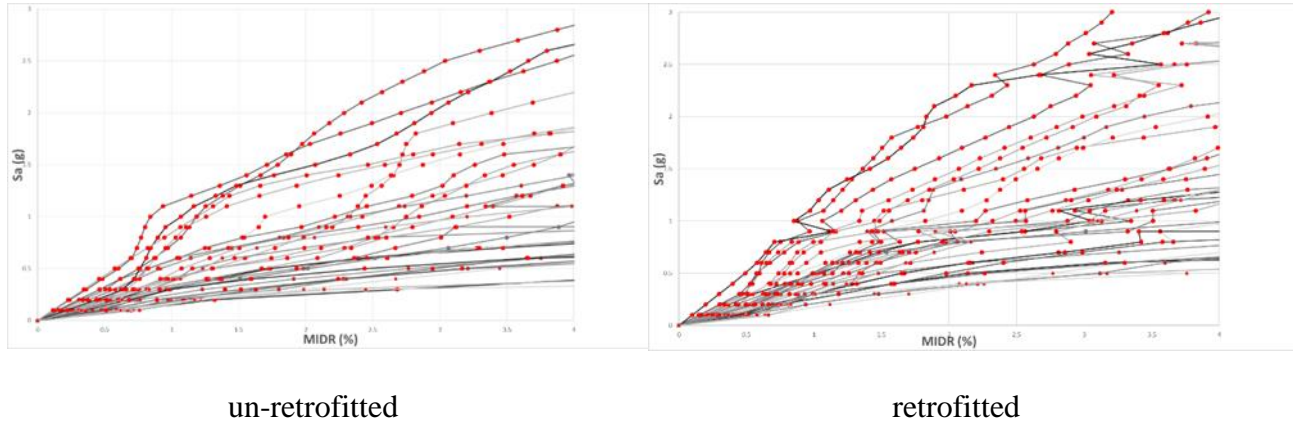un-retrofitted   retrofitted

Fig. 5 IDA curves of the model structures.

To estimate the seismic LCC, the probability of a structure to reach a given damage state needs to be calculated (seismic fragility). A conditional probability lognormal cumulative distribution function is used to relate the structural capacity and the seismic demand as follows [17],

$$P[C < D \ @ \ SI = x] = 1 - \Phi \left| \frac{\ln(\hat{C}/\hat{D})}{\beta_{TOT}} \right| \tag{6}$$

Where C is the structural capacity; D is the structural demand; SI is the seismic intensity hazard; $\Phi[.]$ is the standard normal probability integral; $\hat{C}$ is the median structural capacity for a specific limit state; $\hat{D}$ is the median structural demand; β_{TOT} is the total system collapse uncertainty, which is taken 0.6 based on FEMA P695 [18] recommendation. Fig. 6 shows the comparative fragility curves for the bare and retrofitted frames of the model structures at three damage states: (a) IO, (b) LS, and (c) CP, which assumed to be equivalent to level of maximum inter-story drift ratio (MIDR) of 1%, 2%, and 3%, respectively.
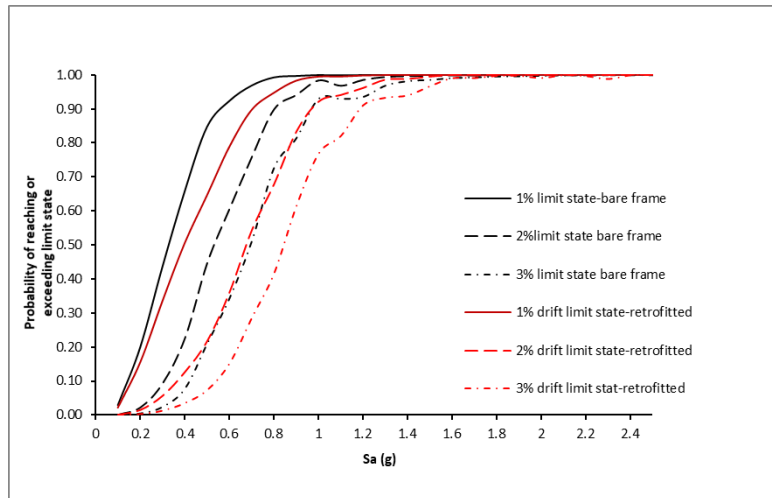
7

Fig. 6 Fragility curves of the bare and retrofitted frames at three damage states.

5. Seismic LCC estimation

In this section, an approximate seismic life cycle cost (LCC) is calculated for the 5-story building to investigate the effect of the retrofit from the economical perspective. LCC primarily depends on the calculation of the damage state probability, which can be obtained through the fragility curves. Wen & Kang [20] suggested that the expected LCC of a structure can be calculated as:

$$E[C_{Lc}] = C_o + \int_0^L E[C_{SD}] \left(\frac{1}{1+\lambda}\right)^t dt = C_o + \propto L\, E[C_{SD}] \tag{7}$$

where C_o is the initial construction cost, L is the service life of the structure, λ is the annual discount rate, and $E[C_{SD}]$ is the annual expected seismic damage cost. The parameters α, q and $E[C_{SD}]$ can be formulated as:

$$\alpha = 1 - exp(-ql)/ql \tag{8}$$

$$q = ln(1 + \lambda) \tag{9}$$

$$[C_{SD}] = \sum_{i=1}^{N} C_i\, P_i \tag{10}$$

where N is the total number of limit-states considered, P_i is the total probability that the structure is in the ith damage state throughout its lifetime, and C_i is the corresponding cost (which includes the cost of damage and its repair). In accordance with the definition of seismic hazard, three structural damage states are used (i.e. N is equal to three) such as IO, LS, and CP, and C_i is assumed to be 30%, 70% and 100%, respectively, of the initial cost of the structure [21]. P_i is given by,

8

$$P_i = P(\Delta_D > \Delta_{C,i}) - P(\Delta_D > \Delta_{C,i+1}) \tag{11}$$

where Δ_D is the earthquake demand and $\Delta_{C,i}$ is the structural capacity, usually represented in terms of drift ratio, defining the ith damage state. The probability of demand being greater than the capacity $\Delta_D > \Delta_{C,i}$ is evaluated based on the values obtained from the fragility calculations discussed earlier.

It is assumed that the annual discount rate is 0.03 and the life service time is 40 years. The initial cost will depend on different parameters including the unit cost of material, labor cost, etc. Based on this, the difference between the LCC and initial cost, which referred to as damage cost, will be used as a reference without specifying a certain value. As the cost of the different elements of the original and retrofitting building has large variability from one location to another and is highly dependent on the construction conditions and many other factors, the ratio of the additional cost of the retrofitting scheme with the damage cost of the un-retrofitted building is used as a basis for comparison. Fig. 7 shows the comparison between the un-retrofitted and retrofitted 5-story building for different cases of the cost of the retrofitting scheme, 2%, 10%, and 20%. These percentages include the LCC of the SC-PC frame. The damage cost has been reduced by almost 33% without considering the cost of the retrofitting scheme. This percentage will be reduced based on the cost of the retrofitting scheme. In the case of the retrofitting scheme costs 2%, 10%, and 20%, respectively, the total damage cost reduction after retrofitting will be 31%, 23%, and 13%. Based on that, the proposed retrofitting scheme in the current study is effective in reducing the total damage cost of the retrofitted building selected in the current study, especially, for the low cost of the SC-PC frames.

a

b

9
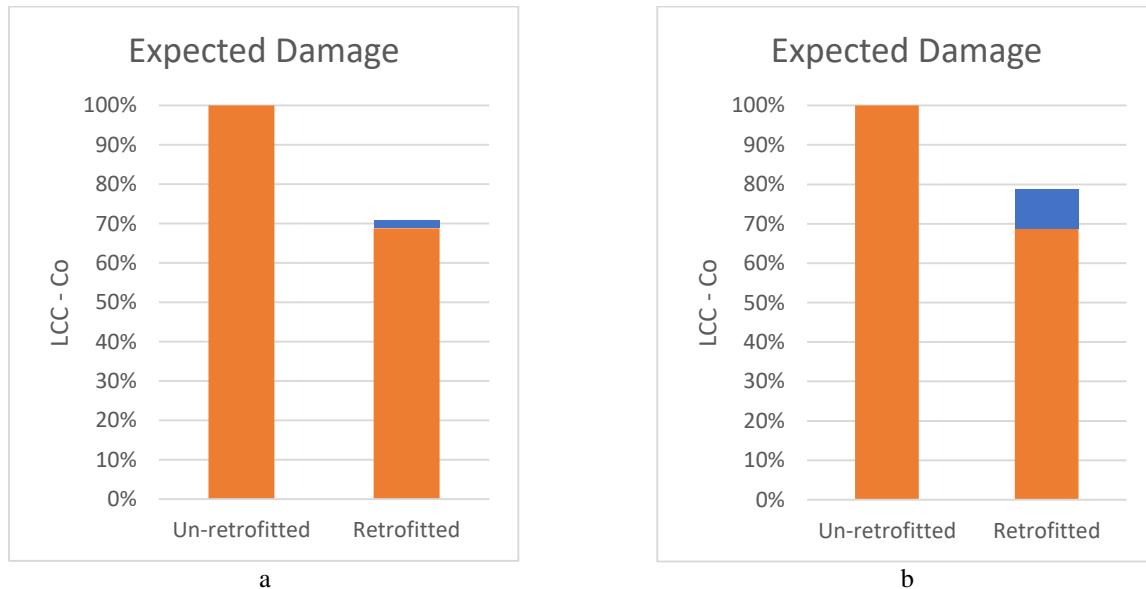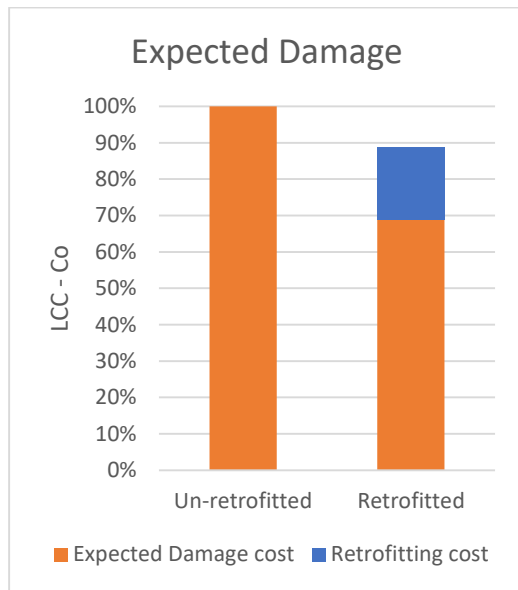
c

Fig. 7 comparison between the bare and retrofitted 5-story building for different cases of the cost of the retrofitting scheme. (a) 2%, (b) 10%, (c) 20%

4. Conclusion

In the current study, a seismic LCC assessment of a retrofitting scheme using SC-PC frames is investigated using a five-story RC building. IDA and fragility curves are constructed and the seismic LCC is estimated to evaluate the effectiveness of the retrofit from an economic perspective. Numerous NLTH analyses are conducted using thirty different ground motion events. The LCC results showed that the proposed retrofit reduced the damage cost (the difference between the LCC and initial cost) by 33 % without considering the cost of the SC-PC frame. This percentage may reach 23% only if the retrofitting frame has a cost of 10% of the total damage cost of the un-retrofitted case. This suggests that the proposed retrofit is suitable for important and expensive structures where the retrofit intervention will not stop the function of the building and where the SC-PC cost is marginal compared to the damage cost of the buildings similar to the buildings investigated in the current study.

5. Acknowledgments

6. References

[1] Chou, C. C., Chen, J. H., Chen, Y. C., and Tsai, K. C. (2006). "Evaluating performance of post-tensioned steel connections with strands and reduced flange plates." *Earthquake Eng. Struct. Dyn.,* 35(9), 1167–1185.

[2] Christopoulos, C., Filiatrault, A., Uang, C. M., and Folz, B. (2002). "Posttensioned energy dissipating connections for moment-resisting steel frames." *J. Struct. Eng.,* 10.1061/(ASCE)0733-9445(2002)128: 9(1111), 1111–1120.

[3] Morgen, B., and Kurama, Y. C. (2004). "A friction damper for posttensioned precast concrete moment frames." PCI J., 49(4), 112–133.

10

[4] Ye Cui, Xilin Lu , Chun Jiang, 2017, Experimental investigation of tri-axial self-centering reinforced concrete frame structures through shaking table tests, Engineering Structures 132 (2017) 684–694.

[5] Roke D, Sause R, Ricles JM, Chancellor B. (2013), Damage-Free Seismic-Resistant Self-Centering Concentrically-Braced Frames, https://nees.org/resources/6727.

[6] Eatherton, M.; Ma, X.; Krawinkler, H.; Deierlein, G.G.; Hajjar, J.F. (2014). Quasi-static cyclic behavior of controlled rocking steel frames. J. Struct. Eng., 140(11).

[7] Cao, Z., Guo, T., Xu, Z. and Lu, S., 2015, Theoretical analysis of self-centering concrete piers with external dissipators. Earthquakes and Structures, An Int'l Journal Vol. 9 No. 6

[8] Wang, B., and Zhu, S., (2018) , 2018), Superelastic SMA U-shaped dampers with self-centering functions, Smart Materials and Structures, https://iopscience.iop.org/article/10.1088/1361-665X/aab52d

[9] Dezfuli, M, A, Dolatshahi, K, M, Mofid, M, Eshkevari, S., S, 2017, Coreless self-centering braces as retrofit devices in steel structures, Journal of Constructional Steel Research, Volume 133, Pages 485-498.

[10] Ryotaro Kurosawa HiroyasuSakataaZheQubTakashiSuyamac, (2019), Precast prestressed concrete frames for seismically retrofitting existing RC frames, Engineering Structures Volume 184, 1 April 2019, Pages 345-354, https://doi.org/10.1016/j.engstruct.2019.01.110

[11] Chancellor N. B., Matthew R. Eatherton 2, David A. Roke 3 and Tuğçe Akbaş, 2014, Self-Centering Seismic Lateral Force Resisting Systems: High Performance Structures for the City of Tomorrow, buildings ISSN 2075-5309 www.mdpi.com/journal/buildings/.

[12] Celik, O., & Sritharan, S. (2004). An Evaluation of Seismic Design Guidelines Proposed for Precast Concrete Hybrid Frame Systems, ISU-ERI-Ames Report ERI-04425, Submitted to the Precast/Prestressed Concrete Manufacturers Association of California, Final report, Iowa State University Of Science And Technology.

[13] American Concrete Institute (ACI), 2014, Building Code Requirements for Structural Concrete (ACI 318-14) and Commentary (ACI 318R-14), Michigan, USA

[14] ASCE/SEI 41-13, (2013). Seismic Evaluation and Retrofit of Existing Buildings. American Society of Civil Engineers, USA.

[15] Sap2000, ver 18, (2015). "Analysis Reference Manual." Computer and Structures, Berkeley, USA.

[16] PEER. Pacific Earthquake Engineering Research (PEER) Center: NGA Database. Retrieved April 8, 2019, from http://peer.berkeley.edu/nga/.

[17] Celik , O.C., Ellingwood , B.R., Seismic risk assessment of gravity load designed reinforced concrete frames subjected to Mid-America ground motions, J. Struct. Eng. 135 (4) (2009) 414–424, http://dx.doi.org/10.1061/(ASCE)0733-9445(2009) 135:4(414).

[18] FEMA P695, Quantification of Building Seismic Performance Factors, Federal Emergency Management Agency, Washington (DC, USA), 2009.

[19] NourEldin M., Naim A., Kim jK, 2019, Seismic retrofit of a structure using self-centring precast concrete frames with enlarged beam ends, Magazine of Concrete Research, https://doi.org/10.1680/jmacr.19.00012.

[20] Wen, Y. K., Kang, Y. J. (2001). Minimum building life cycle cost design criteria I: Methodology. Journal of Structural Engineering (ASCE); 127(3):330–337

[21] Fragiadakis, M., Lagaros, N. D., Papadrakakis, M. (2006). Performance-based multi objective optimum design of steel structures considering life-cycle cost. Struct Multidiscip Optimiz. 32. 1–11.